JOURNAL OF SOLID STATE CHEMISTRY **121,** 319–323 (1996)
ARTICLE NO. 0043

Stabilization of the 8-8-20 Structure-Type in $La_{8-x}Ca_xCu_{8-y}Ni_yO_{20}$

G. L. Roberts, R. J. Cava, S. A. Carter, J. J. Krajewski, and W. F. Peck Jr.

AT & T Bell Laboratories, Murray Hill, New Jersey 07974

Received July 27, 1995; in revised form September 29, 1995; accepted October 5, 1995

The 8-8-20 oxygen deficient perovskite occurs in the La–Sr–Cu–O chemical system near composition $La_{6.4}Sr_{1.6}Cu_8O_{20}$. Here we show that this structure can be stabilized in the La–Ca–Cu–Ni–O system based on the composition $La_{6.4}Ca_{1.6}Cu_6Ni_2O_{20}$. In the new system, a wider variation of hole concentration is possible. Transport properties of the series reveal an insulator to metal transition as a function of increasing Ca (hole) concentration. Phase stability studies suggest that Ni preferentially substitutes for octahedrally coordinated copper. © 1996 Academic Press, Inc.

INTRODUCTION

A renewed interest in the search for mixed-valence copper, Cu(II)–Cu(III), compounds has prompted the investigation of oxygen deficient $La_{8-x}Sr_xCu_{8-y}O_{20}$ perovskites of the 8-8-20 structure type. The metallic behavior, as well as three-dimensionality of the crystal structures, is of interest due to similarities with copper-oxide superconductors. The 8-8-20 phase is derived by introducing oxygen vacancies into $LaCuO_3$, from which a variety of oxygen deficient perovskites may be obtained. There are at least six known types, but $La_4BaCu_5O_{13}$ is most often the choice of comparison for 8-8-20 (1–4). $La_4BaCu_5O_{13}$ contains formally 3 Cu^{2+} and 2 Cu^{3+}. The ideal structure has 3-CuO_6 elongated octahedra and 2-CuO_5 square based pyramids with an oxygen vacancy in each unit cell. The 8-8-20 compounds and related three-dimensional oxygen deficient perovskites have not been made superconducting probably due to their three-dimensional character (5–7). However, applicability of the compounds has been realized in the area of thin film growth. Epitaxial thin films of the isotropic metallic oxide $La_{8-x}Sr_xCu_8O_{20}$ can be grown (8). Isotropic materials are ideal for device fabrication because the devices can be grown in any direction.

The majority of work reported on these systems has concentrated on strontium-doped compounds. A description of the unit cell for $La_{8-x}Sr_xCu_8O_{20}$ was previously discussed in detail (6, 7, 9). The stoichiometric 8-8-20 tetragonal unit cell has lattice parameters $a \cong a_p\,2\sqrt{2}$ and $c \cong a_p$. The structure consists of 2-CuO_6 octahedra, 4-CuO_5 pyramids, and 2-CuO_4 square planar units. The $[Cu_8O_{20}]_\infty$ framework is an ordered oxygen deficient perovskite, with anionic vacancies, that consists of rows of corner-sharing CuO_6 octahedra and CuO_5 pyramids running along c, interconnected by rows of CuO_4 square planar groups (8, 10). The octahedra, pyramids, and square planar groups form hexagonal tunnels in which the La^{3+} and Sr^{2+} ions are located. The metallic behavior of the compound is attributed to the mixed-valence of Cu(II)–Cu(III).

Er-Rakho *et al.* (7) examined substitution of Sr^{2+} at the La^{3+} site in $LaCuO_3$ for $La_{8-x}Sr_xCu_8O_{20-\delta}$ ($x = 1.28$ to 1.92; $\delta = 0.08$ to 0.32) and found that a general composition of $x = 1.6$ gave the stable 8-8-20 structure type. Michel *et al.* (5) reported the electron transport and magnetic properties of the oxygen deficient copper perovskite $La_{8-x}Sr_xCu_8O_{20-\delta}$ ($1.28 \le x \le 1.92$) and found the conductivity of the compounds to be metallic. Genouel *et al.* (10) isolated two series of iron-substituted cuprates with the tetragonal $La_{6.4}Sr_{1.6}Cu_8O_{20}$ oxygen deficient perovskite structure: $La_{6.4}Sr_{1.6}Cu_{8-x}Fe_xO_{20}$ ($0 \le x \le 1.20$) and $La_{6.4-x}Sr_{1.6+x}Fe_xO_{20}$ ($0 \le x \le 2$). Both compounds are metallic conductors. A variety of other oxygen deficient strontium-doped lanthanum cuprates are being explored (4, 9, 11–13).

It is well known that transition metals can be substituted for copper in superconducting cuprates. Our interest in developing new electrodes/electrocatalysts for oxygen evolution and oxygen reduction studies led to the substitution of Ca^{2+} at the La^{3+} site and Ni^{2+} at the Cu^{2+} site in the 8-8-20 structure type.

Herein described are the substitutional, transport, and magnetic properties of two series of nickel-substituted oxides, $La_{8-x}Ca_xCu_6Ni_2O_{20}$ and $La_{6.4}Ca_{1.6}Cu_{8-y}Ni_yO_{20}$, which belong to the 8-8-20 family of compounds.

EXPERIMENTAL

Synthesis and Characterization

The two series of compounds, $La_{8-x}Ca_xCu_6Ni_2O_{20}$ ($1 \le x \le 2.2$) and $La_{6.4}Ca_{1.6}Cu_{8-y}Ni_yO_{20}$ ($1 \le y \le 2$), were prepared via solid state synthesis from the corresponding oxide and carbonate precursors. Starting materials consisted of previously dried La_2O_3, $CaCO_3$, CuO, and NiO.

0022-4596/96 $18.00

Stoichiometric amounts of the starting materials were mechanically ground (agate mortar and pestle) and long heating times were employed to insure sample homogeneity. The samples were initially fired in air at 1000°C. The final heating was performed in an oxygen atmosphere at 1025°C. The powders were pressed into $\frac{1}{2}$-in. diameter pellets (1.50 g) for the final heating stage. Pellets were well densified but were not in excess of 90% of theoretical density.

Sample purity and lattice constants were determined from the X-ray powder diffraction patterns obtained using either a Rigaku or Philips diffractometer (Cu$K\alpha$ radiation, $20° \leq 2\Theta \leq 60°$, room temperature). Data were collected at a scan rate of 0.03°/sec. Lattice parameters were determined using the NRCVAX program package (14).

Resistivity measurements were performed on single-phase polycrystalline pellets over the temperature range 300–4 K using a standard four-probe d.c. technique. Temperature-dependent magnetic susceptibility was measured using a commercial Quantum Design SQUID magnetometer at an applied magnetic field of 2000 G.

Oxygen content for several representative samples was determined thermogravimetrically using a model 2950 thermogravimetric analyzer. Samples were heated to 900°C at a rate of 5°/min and isotracked for 30 min at 900°C. The samples were reduced to La_2O_3 + CaO + *TM* (*TM* = Ni, Cu) in a mixture of 15% Hydrogen: 85% Nitrogen. Analysis revealed oxygen contents of 20.1(1) per formula unit, which agrees with the structural model.

TABLE 1
Compounds Tested for Stability Limits of 8-8-20 Structure Type

Compound	Lattice parameter a =, c = (Å)	Average transition metal valence	ρ_{300}/m$\Omega \cdot$cm
$La_{5.8}Ca_{2.2}Cu_{6.0}Ni_{2.0}O_{20}$	10.688(9), 3.860(3)	2.275	1.11
$La_{6.0}Ca_{2.0}Cu_{6.0}Ni_{2.0}O_{20}$	10.706(4), 3.864(2)	2.250	0.95
$La_{6.1}Ca_{1.9}Cu_{6.0}Ni_{2.0}O_{20}$	10.700(2), 3.866(2)	2.237	0.95
$La_{6.4}Ca_{1.6}Cu_{6.0}Ni_{2.0}O_{20}$	10.719(8), 3.863(3)	2.20	0.91
$La_{6.7}Ca_{1.3}Cu_{6.0}Ni_{2.0}O_{20}$	10.739(3), 3.853(1)	2.162	2.63
$La_{7.0}Ca_{1.0}Cu_{6.0}Ni_{2.0}O_{20}$	10.749(9), 3.866(3)	2.125	2.86
$La_{6.4}Ca_{1.6}Cu_{6.5}Ni_{1.5}O_{20}$	10.719(9), 3.862(3)	2.20	
$La_{6.4}Ca_{1.6}Cu_{7.0}Ni_{1.0}O_{20}$	10.746(2), 3.863(1)	2.20	1.67
$La_{6.4}Ca_{1.6}Cu_{7.5}Ni_{0.5}O_{20}$	10.804(1), 3.847(1)	2.20	2.38

RESULTS AND DISCUSSION

Powder X-Ray Diffraction

Single-phased materials were obtained for $1 \leq x \leq 2.2$ for $La_{8-x}Ca_xCu_6Ni_2O_{20}$ and $1 \leq y \leq 2$ for the series $La_{6.4}Ca_{1.6}Cu_{8-y}Ni_yO_{20}$. Analysis indicated that the oxygen content is approximately constant for the as-synthesized samples. Powder X-ray diffraction patterns of the samples further indicated that the samples could be indexed with a tetragonal cell with parameters $a \cong 2a_p\sqrt{2}$, $c \cong a_p$ (a = 10.72 Å, c = 3.86 Å and a = 10.75 Å, c = 3.86 Å for the calcium-doped and nickel-substituted samples, respectively). The lattice parameters for both series are listed in Table 1.

Analysis of the lattice parameter c (Å) as a function of calcium and nickel composition indicates that it does not vary significantly over the range of compositions investigated. For the nickel-substituted series, with increasing nickel concentration, the lattice parameter a decreases until a composition of x = 1.5 is reached, at which time it remains constant even for $x = 2$. A nearly linear decrease in a is observed in the case of increasing calcium composition, with the exception of x = 1.9.

Investigation of the limits of the solid solution for the La : Ca composition in $La_{8-x}Ca_xCu_6Ni_2O_{20}$ revealed that the structure type could be made single phase for $1 \leq x \leq 2.2$. This implies that we have a range of 1.2 holes distributed over the 8 metal sites (or 0.15 holes/metal), from an average Cu, Ni valence of 2.125 at x = 1.0, to an average valence of 2.275 at x = 2.2.

If nickel could only be substituted at the octahedral Cu sites, then a maximum value of y = 2.00 is expected for $La_{6.4}Ca_{1.6}Cu_{8-y}Ni_yO_{20}$. The samples tested to verify the stability were for y = 0.5 to 2.5. The X-ray patterns for y = 1.0, 1.5, and 2.0 did not contain impurity peaks; y = 0.5 and 2.5 were not single phase. Therefore it takes a minimum of 1 Ni to stabilize the structure type, and the maximum Ni content observed is consistent with the hypothesis of octahedral site substitution only. The range of the solid solution, with respect to nickel substitution, is therefore $La_{6.4}Ca_{1.6}Cu_{8-y}Ni_yO_{20}$ ($1 \leq y \leq 2$).

We also investigated the solid solution range for Y-doped $La_{8-x}Y_xCu_6Ni_2O_{20}$. The structure type transforms from tetragonal 8-8-20 to a nearly perfect cubic perovskite even at low Y contents. $La_7YCu_6Ni_2O_{24-\delta}$, synthesized under oxygen for 58 hr, contained one impurity peak at 31.3° $2 - \Theta$ (15% of the largest peak) and a cubic cell size of approximately 3.843 Å. The $La_6Y_2Cu_6Ni_2O_{24-\delta}$ sample was prepared in an oxygen atmosphere, annealed an additional 12 hr but single-phase material was not obtained. The X-ray pattern consisted of one regular perovskite phase with a = 3.851 Å along with a second phase. Attempts to incorporate even more Y, i.e., to make $La_4Y_4Cu_6Ni_2O_{20}$, resulted in the formation of $Y_2Cu_2O_5$ along with a cubic perovskite phase.

$La_{6.4}Ca_{1.6}Cu_{6.0}M_{2.0}O_{20}$ (*M* = Fe, Co, Ru, Pd) analogs were also explored. Starting materials consisted of previously dried La_2O_3, $CaCO_3$, CuO, Fe_2O_3, Co_3O_4, PdO, and RuO_2. Stoichiometric amounts of the starting materials were mechanically ground (agate mortar and pestle) and

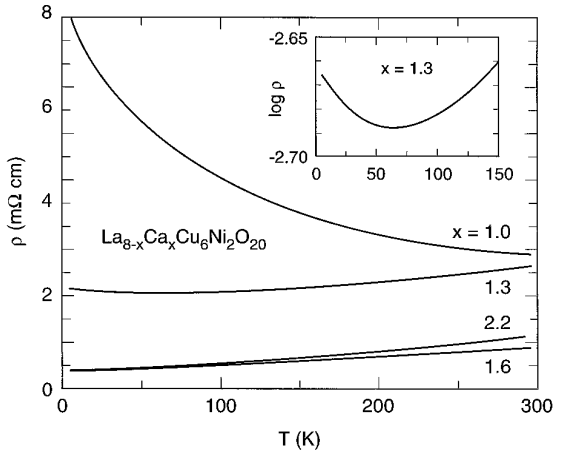

FIG. 1. Resistivity ρ ($\Omega \cdot$ cm) versus T (K) for the series $La_{8-x}Ca_xCu_6Ni_2O_{20}$ ($1 \leq x \leq 2.2$).

long heating times were employed to insure sample homogeneity. The samples were initially fired in air at 1000°C. The final heating was performed in an oxygen atmosphere at 1025°C. The powders were pressed into $\frac{1}{2}$-in. diameter pellets (1.50 g) for the final heating stage.

In the case of the iron- and strontium-substituted 8-8-20 analog, as reported by Genouel *et al.* (10), iron can occupy both the octahedral and pyramidal sites (86% and 14%, respectively). We were able to verify the existence of the iron-substituted compound in the 8-8-20 structure type with $x = 2$ at approximately 90% purity.

The $La_{6.4}Ca_{1.6}Cu_{6.0}Ru_{2.0}O_{20}$ X-ray pattern suggested a relation with the 8-8-20 structure type but was multiple phase, while that of $La_{6.4}Ca_{1.6}Cu_{6.0}Co_{2.0}O_{20}$ was clearly that of the 8-8-20 type. The samples were further heated at higher temperature under oxygen but never formed an 8-8-20 structure type compound that was single phase. Four-probe resistance measurements indicated that the compounds are highly conductive oxides. Substitution of Pd resulted in a multiple-phase sample.

Transport Properties

Samples were tested for superconductivity down to 4 K by a.c. susceptibility. Superconductivity was not observed. Resistivity as a function of temperature was measured, for both series, on single-phase polycrystalline pellets of $La_{8-x}Ca_xCu_6Ni_2O_{20}$ and $La_{6.4}Ca_{1.6}Cu_{8-y}Ni_yO_{20}$ in the temperature range 300–4 K. Room temperature resistivity measurements for the different compositions are listed in Table 1.

The temperature dependence of the resistivity of $La_{8-x}Ca_xCu_6Ni_2O_{20}$ ($x = 1.0$ to 2.2) and $La_{6.4}Ca_{1.6}Cu_{8-y}Ni_yO_{20}$ ($y = 1.0$ to 2.0) samples are shown in Figs. 1 and 2, respectively. For the series of samples $La_{8-x}Ca_xCu_6Ni_2O_{20}$ metallic behavior is observed for $x = 1.6$, 1.9, 2.0, and 2.2. At the lower doping level of $x = 1.3$ there is a slight upturn in the resistivity that moves to higher temperature with decreasing level of dopant to $x = 1.0$. The magnitude of the resistivity also increases. A plot of the logarithm of resistivity as a function of $1/T$ shows that the slope indeed changes sign at a temperature $T_{(\text{metal–insulator})}$ which increases with decreasing x. In the case of the $La_{6.4}Ca_{1.6}Cu_{8-y}Ni_yO_{20}$ series, metallic behavior is observed for $y = 2$, whereas the resistivity tends toward insulating for the $y = 1.0$ doped sample. It is evident from log ρ versus T plots that the conductivity of the samples goes through a metal–insulator transition as the y doping level exceeds 1.0. Michel *et al.* reported the electron transport and magnetic properties of $La_{8-x}Sr_xCu_8O_{20-\delta}$ ($1.28 \leq x \leq 1.92$) and found the compounds to be of metallic character at low temperature (5).

The magnetic susceptibility, χ, of the $La_{8-x}Ca_xCu_6Ni_2O_{20}$ series is shown in Fig. 3. Below 200 K, χ can be fit to the Curie–Weiss form $\chi_0 + C/(T + \Theta)$, where χ_0 is the temperature-independent contribution, C is the Curie constant, and Θ is the Curie temperature. The χ_0's are in the range of $1.5(0.2) \times 10^{-4}$ emu/mole formula unit for the four metallic samples, $2.2 \geq x \geq 1.6$. This value decreases to $1.1(0.1) \times 10^{-4}$ emu/mole f.u. and $0.7(0.1) \times 10^{-4}$ emu/mole f.u. for the $x = 1.3$ and 1.0 materials, respectively, presumably due to the decrease of the density of carriers at the Fermi surface. The analysis of Curie–Weiss behavior is complicated by the mixed valent nature of both the Cu and Ni spins; nonetheless, there are some trends. The Curie term, C, is 0.05(0.02) emu K/mole f.u. for the metallic materials which indicates that only a small percentage of the Cu and Ni spins behave as local moments. A significant increase in local moment character occurs as the material becomes insulating, with $C \approx 0.35(0.02)$ emu K/mole f.u. for $x = 1.0$. Finally, the antiferromagnetic Θ values increase

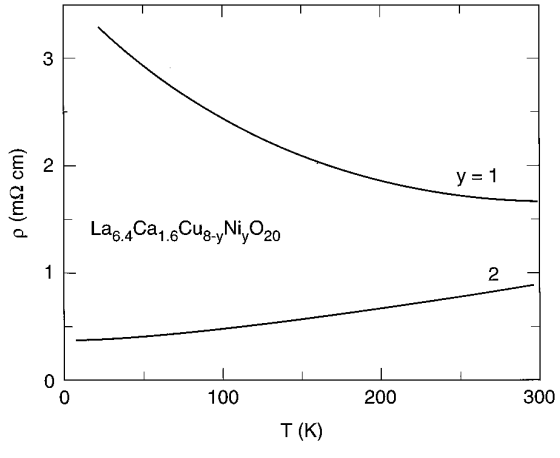

FIG. 2. Resistivity ρ ($\Omega \cdot$ cm) versus T (K) for the series $La_{6.4}Ca_{1.6}Cu_{8-y}Ni_yO_{20}$ ($1 \leq y \leq 2$).

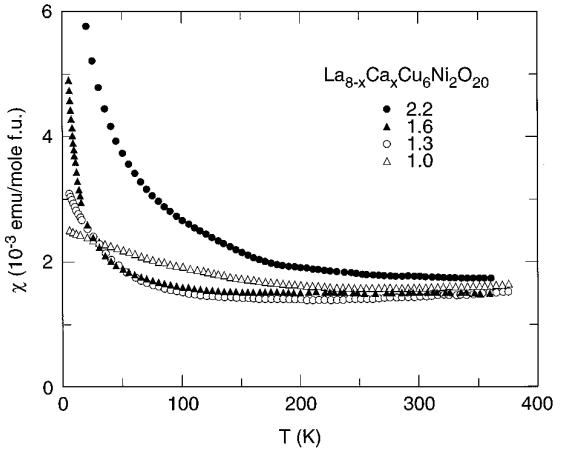

FIG. 3. Magnetic susceptibility as a function of temperature for the series $La_{8-x}Ca_xCu_6Ni_2O_{20}$ ($1 \leq x \leq 2.2$).

from 3 to 180 K with decreasing x. Below 200 K, we observe a small rise in χ in some of the samples which may indicate small amounts of inhomogeneity or impurities.

Figure 4 shows a plot of magnetic susceptibility, χ, as a function of temperature for the $La_{6.4}Ca_{1.6}Cu_{8-y}Ni_yO_{20}$ series. Antiferromagnetic ordering at temperatures below 20 K occurs for the $y = 1.0$ sample. The temperature-independent contributions of $7.4(1) \times 10^{-4}$ emu/mole f.u. and the Curie terms of 0.26(0.02) emu K/mole f.u. are comparable for both materials. The inset of Fig. 4 shows the large change in the Curie constant C which occurs during the transition from metallic ($y = 2$) to insulating ($y = 1.0$) behavior. These results are similar to those observed for the $x = 1.0$ insulating sample (Fig. 1) and suggest that as the material becomes more insulating, a larger fraction of the spins behave as local moments. As a consequence there is an increase in C and a decrease in χ_0, eventually leading to long range antiferromagnetic order.

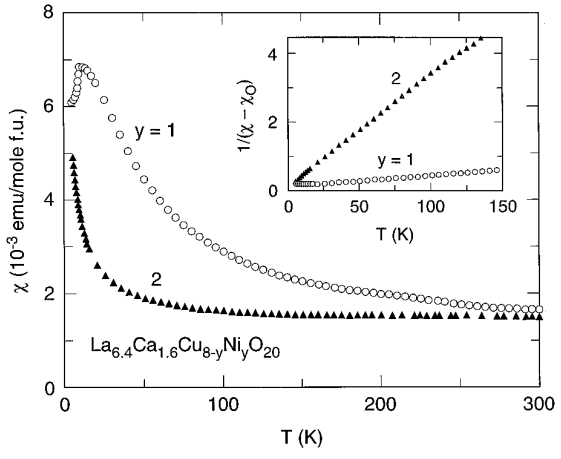

FIG. 4. Magnetic susceptibility as a function of temperature for the series $La_{6.4}Ca_{1.6}Cu_{8-y}Ni_yO_{20}$ ($1 \leq y \leq 2$).

Because both Ni and Cu commonly occur in formal valences between 2 and 3 in perovskite oxides, we cannot assign specific valences. (The average valence of the transition metal is 2.20 in analogous $La_{6.4}Sr_{1.6}Cu_8O_{20}$.) The data indicate that (i) the resistivity decreases as the average transition valence (a measure of hole concentration) increases and (ii) at fixed average metal valence, as the Ni content increases the resistivity once again decreases. There are at least two possible origins for the observed behavior. First, at the Ni_2 composition all octahedral sites are filled and there is less disorder and scattering, so the resistivity decreases. Second, there could be a subtle redistribution of the holes occurring as the Ni/Cu ratio is changed.

The presence of magnetic ordering for $La_{6.4}Ca_{1.6}Cu_7Ni_{1.0}O_{20}$ suggests that in that composition a subset of the Cu sites has a valence near 2+. Band structure calculations would possibly be helpful in determining the charge distribution between Cu and Ni.

CONCLUSIONS

The solid solution domains of $La_{8-x}Ca_xCu_{8-y}Ni_yO_{20}$ have been determined for calcium-doped and nickel-substituted compounds. Single-phase 8-8-20 type lanthanum-copper-nickelates can be prepared for $La_{8-x}Ca_xCu_6Ni_2O_{20}$ ($1 \leq x \leq 2.2$) and $La_{6.4}Ca_{1.6}Cu_{8-y}Ni_yO_{20}$ ($1 \leq y \leq 2$). The maximum level of Ni substitution that can be achieved, while maintaining the 8-8-20 structure type, clearly indicates that Ni preferentially substitutes at the octahedral Cu site. Substitution of Fe, Co, Ru, and Pd at the octahedral Cu site did not result in single-phase material. Temperature-dependent resistivity measurements indicate that $La_{8-x}Ca_xCu_6Ni_2O_{20}$ goes through a transition from insulating ($x \leq 1.3$) to metallic ($x \geq 1.3$). Metallic behavior is observed for $y = 2$, whereas the resistivity tends toward insulating for the $y = 1.0$ and 1.5 $La_{6.4}Ca_{1.6}Cu_{8-y}Ni_yO_{20}$ series.

REFERENCES

1. P. K. Davies and C. M. Katzan, *J. Solid State Chem.* **88,** 368 (1990).
2. P. Hagenmuller, M. Pouchard, and J. C. Grenier, *Solid State Ionics* **43,** 7 (1990).
3. C. Michel, L. Er-Rakho, and B. Raveau, *Mater. Res. Bull.* **20,** 667 (1985).
4. K. Otzschi, A. Hayashi, Y. Fujiwara, and Y. Ueda, *J. Solid State Chem.* **105,** 573 (1993).
5. C. Michel, L. Er-Rakho, and B. Raveau, *J. Phys. Chem. Solids* **49,** 451 (1988).
6. R. J. Cava, H. W. Zandbergen, R. B. Van Dover, J. J. Krajewski, T. Siegrist, W. F. Peck Jr., R. S. Roth, and R. J. Felder, *J. Solid State Chem.* **109,** 345 (1994).

7. L. Er-Rakho, C. Michel, and B. Raveau, *J. Solid State Chem.* **73,** 514 (1988).
8. C.-B. Eom, J. M. Phillips, and R. J. Cava, "Materials Research Society Symposium Proceedings" Vol. 341, p. 229 (1994).
9. W. T. Fu, R. J. Drost, D. J. W. Ijdo, and E. Frikkee, *Mater. Res. Bull.* **29,** 629 (1994).
10. R. Genouel, C. Michel, N. Nguyen, M. Hervieu, and B. Raveau, *J. Solid State Chem.* **115,** 469 (1995).
11. W. T. Fu, D. J. W. Ijdo, and R. B. Helmholdt, *Mater. Res. Bull.* **27,** 287 (1992).
12. K. Otzschi and Y. Ueda, *J. Solid State Chem.* **107,** 149 (1993).
13. K. Otzschi, K. Koga, and Y. Ueda, *J. Solid State Chem.* **115,** 490 (1995).
14. E. J. Gabe, Y. Le Page, J.-P. Charland, F. L. Lee, and P. S. White, *J. Appl. Crystallogr.* **22,** 384 (1989).